

Section Nine

Plate Bending

Plate bending using *hp*-Clouds and Trefftz-based enrichment

Carlos Tiago¹ and Vitor M.A. Leitão²

¹ Universidade Técnica de Lisboa, Instituto Superior Técnico
Av. Rovisco Pais, 1049-001 Lisboa, Portugal.
E-mail: carlos.tiago@civil.ist.utl.pt.

² Universidade Técnica de Lisboa, Instituto Superior Técnico
Av. Rovisco Pais, 1049-001 Lisboa, Portugal.
E-mail: vitor@civil.ist.utl.pt.

Keywords: *meshless*, *hp*-Cloud, plate bending, Trefftz.

Abstract The aim of the present work is to examine the performance of the *hp*-Cloud method in the analysis of thin plates (Kirchhoff's theory). The partition of unity (POU) is constructed using the Shepard functions. The enrichment is made through Trefftz functions, i.e., functions that are homogeneous solutions of the governing equation of the problem. As this approximation does not possess the Kronecker-delta property, the essential boundary conditions are relaxed and imposed via Lagrange multiplier method.

Introduction

The mesh requirements usually associated with traditional finite element methods (FEM) may be reduced in, basically, two ways: by using boundary-type of formulations, such as boundary element methods (BEM) and Trefftz techniques, amongst others; or by establishing approximations based on nodes instead of elements. This latter approach is behind most of the *meshless* methods that have been presented in recent years such as SPH method, the DEM, the EFG method, and the RKPM. For a review see Belytschko *et al* [2]. Using the concept of the partition of unity, other methods such as the Partition of Unity FEM [1] and the *hp*-Cloud method [3] were devised. Except for the SPH method, which uses collocation, all other methods require a background cell structure in order to integrate the variational form of the problem. Alternative meshless collocation procedures (which totally avoid integrations) were used by the authors in the fields of Radial Basis Functions (RBF) [5] and Trefftz Methods [6] but will not be discussed here.

The *hp*-Cloud method may be seen to be more flexible [3] than most of the other meshless methods due to the possibility of improving accuracy, without remeshing, in two ways: *h*-type refinement whereby extra points (i.e. clouds centers) are added to the domain; *p*-type refinement whereby the approximate solution is enriched by adding specific functions (polynomials, trigonometric, etc) to some (or all) nodes. In this method, the partition of unity is constructed using the minimal set of monomials that result from the application of moving least squares (MLS) [2], i.e., the Shepard functions.

In a previous work of Garcia *et al.* [4] the *hp*-clouds method was applied to Mindlin's thick plate model where shear locking was avoided by using *p* refinement. In the present work the method is applied to the thin plate model. The thin plate model uses differential operators (in the expression of the internal energy) of higher order than those occurring for the thick plate and this poses some difficulties as compared to the thick plate implementation of the *hp*-clouds method. Enrichment is achieved with functions that satisfy *a priori* the Lagrange homogeneous equation. The final governing system is obtained by enforcing stationarity on a functional including the potential energy and Lagrange multipliers.

Plate bending equations

The main equations for the analysis of thin plates are now briefly described on the plate of uniform thickness, t , domain Ω , kinematic boundary $\Gamma_w \cup \Gamma_{\frac{\partial w}{\partial n}}$ and static boundary $\Gamma_{M_n} \cup \Gamma_{V_n}$, where the subscript n stands for outside normal.

Equilibrium: Collecting the bending moments and shear forces in the vectors $\mathbf{M}^T = \{ M_{xx} \ M_{yy} \ M_{xy} \}$ and $\mathbf{Q}^T = \{ Q_x \ Q_y \}$, respectively, the equilibrium equations can be written as $\mathbf{L}^T \mathbf{M} - \mathbf{Q} = \mathbf{0}$ and $\nabla^T \mathbf{Q} + \bar{p} = 0$ where \bar{p} is the transverse load, \mathbf{L} and ∇ are the usual differential operators.

Applying the ∇^T to both sides of the first equation and substituting in the second it follows $(\mathbf{L}\nabla)^T \mathbf{M} + \bar{p} = 0$ and $(\mathbf{L}\nabla)^T = \left[\frac{\partial^2}{\partial x^2} \quad \frac{\partial^2}{\partial y^2} \quad 2\frac{\partial^2}{\partial x \partial y} \right]$.

Compatibility: Collecting the curvatures and shear strains in the vectors $\boldsymbol{\chi}^T = \{ \chi_{xx} \ \chi_{yy} \ 2\chi_{xy} \}$ and $\boldsymbol{\gamma}^T = \{ \gamma_{xz} \ \gamma_{yz} \}$, respectively, the compatibility equations can be written as $\boldsymbol{\chi} = \mathbf{L}\boldsymbol{\theta}$ and $\boldsymbol{\gamma} = \nabla w + \boldsymbol{\theta}$ where $\boldsymbol{\theta}^T = \{ \theta_x \ \theta_y \}$ is a vector containing the rotations. Neglecting the shear strains, $\boldsymbol{\gamma} = \mathbf{0}$, the rotations vector and the curvatures are given by $\boldsymbol{\theta} = -\nabla w$ and $\boldsymbol{\chi} = -(\mathbf{L}\nabla)w$.

Constitutive relations: Assuming a plane stress state for each fiber, the constitutive relations are given by $\mathbf{M} = \mathbf{D}\boldsymbol{\chi}$ where \mathbf{D} represents the stiffness.

Boundary conditions: The two appropriate boundary conditions of each boundary point are $w = \bar{w}$ or $V_n = \bar{V}_n$ and $\frac{\partial w}{\partial n} = \bar{\frac{\partial w}{\partial n}}$ or $M_n = \bar{M}_n$ where V is the effective shear force.

hp-Clouds approximations

The notation used here follows closely the work of Garcia *et al.* [4]. In the following, only a brief description of the functions used is given. Consider an arbitrary set of N points $\mathbf{x}_\alpha \in \Omega, \alpha = 1, \dots, N$. Associated with each of these points there is a open set called domain of influence or *cloud*, $\omega_\alpha = \{\mathbf{x} \in \Omega; \|\mathbf{x} - \mathbf{x}_\alpha\| \leq h_\alpha\}$. These *clouds* are chosen in such a way that they form a finite open covering of the domain, $\mathfrak{S}_N = \{\omega_\alpha\}_{\alpha=1}^N$. Associated with the *clouds* there is a set of functions $\mathcal{L}_N = \{\psi\}_{\alpha=1}^N$ that form a partition of unity. In this work Shepard functions are used to build the POU:

$$\psi_\alpha(\mathbf{x}) = \frac{\mathcal{W}_\alpha(\mathbf{x})}{\sum_\beta \mathcal{W}_\beta(\mathbf{x})} \quad \beta \in \{\gamma : \mathcal{W}_\gamma(\mathbf{x}) \neq 0\} \tag{1}$$

The weight function appearing in (1) depends only on the normalized radius or distance $r_\alpha = \frac{\|\mathbf{x} - \mathbf{x}_\alpha\|}{h_\alpha}$ between the point \mathbf{x} under consideration and the point \mathbf{x}_α . In this paper the following quartic spline was used:

$$\mathcal{W}(r_\alpha) = \begin{cases} 1 - 6 r_\alpha^2 + 8 r_\alpha^3 - 3 r_\alpha^4 & \text{for } 1 > r \geq 0 \\ 0 & \text{for } r \geq 1 \end{cases} \tag{2}$$

In the *hp-cloud* method, higher order approximations (than that given by the POU) are made possible through the enrichment of the POU functions (1) by a suitable set of functions, $L_{\alpha i}(\mathbf{x}), i = 1, \dots, M_\alpha$. Thus, the approximation $\tilde{u}(\mathbf{x})$ of $u(\mathbf{x})$ on each point can be written as

$$\tilde{u}(\mathbf{x}) = \sum_{\alpha=1}^N \psi_\alpha(\mathbf{x}) \left\{ u_\alpha + \sum_{i=1}^{M_\alpha} L_{\alpha i}(\mathbf{x}) b_{\alpha i} \right\} = \mathbf{\Phi} \mathbf{u} \tag{3}$$

where u_α and $b_{\alpha i}$ are the unknown coefficients.

As the number of enrichment functions M_α depends on the *cloud* under consideration, it is easy to use different p refinement on different parts of the domain.

Amongst the many possible enrichment functions, the one chosen in this work stems from the so-called T (or Trefftz)-functions which, for thin plates, may be given by

$$w_h = \Re [\bar{\zeta} \Phi + \chi] \tag{4}$$

where $\zeta = x + iy, \bar{\zeta} = x - iy$ and $\Phi = \Phi(\zeta)$ and $\chi = \chi(\zeta)$ are complex valued series. By choosing

$$\Phi(\zeta) = \sum_{i=1}^M a_i(\zeta)^i \quad \text{and} \quad \chi(\zeta) = \sum_{i=2}^M b_i(\zeta)^i, \tag{5}$$

the terms of equation (4) constitute the enrichment functions used in this work which may be written as $\mathbf{L}_\alpha(\mathbf{x}) = [\mathbf{L}_1 \quad \mathbf{L}_2 \quad \dots \quad \mathbf{L}_{M_\alpha}]$ where $\mathbf{L}_1 = [r^2]$ and $\mathbf{L}_i = [r^2 \Re(\zeta)^{i-1} \quad -r^2 \Im(\zeta)^{i-1} \quad \Re(\zeta)^i \quad -\Im(\zeta)^i]$ with $r^2 = x^2 + y^2$ and $i = 2, 3 \dots M_\alpha$.

Governing system

A generalization of the Principle of Minimum Potential Energy (which includes the kinematic boundary conditions through the inclusion of Lagrange multipliers [7]) was used. Note that, in this case, the solution is not obtained by minimization of the variational principle but by enforcing stationarity conditions.

$$\begin{aligned} \Pi_I = & \frac{1}{2} \int_{\Omega} \boldsymbol{\chi}^T \mathbf{D} \boldsymbol{\chi} d\Omega - \int_{\Omega} \bar{p} w d\Omega - \int_{\Gamma_{\bar{V}_n}} \bar{V}_n w d\Gamma_{\bar{V}_n} \\ & - \int_{\Gamma_{\bar{M}_n}} \bar{M}_n \left(-\frac{\partial w}{\partial n} \right) d\Gamma_{\bar{M}_n} - \int_{\Gamma_{\bar{w}}} \lambda^w (w - \bar{w}) d\Gamma_{\bar{w}} \\ & - \int_{\Gamma_{\frac{\partial w}{\partial n}}} \lambda^{\frac{\partial w}{\partial n}} \left(\frac{\partial w}{\partial n} - \bar{\frac{\partial w}{\partial n}} \right) d\Gamma_{\frac{\partial w}{\partial n}} \end{aligned} \quad (6)$$

where λ^w and $\lambda^{\frac{\partial w}{\partial n}}$ are Lagrange multipliers.

In this work the Lagrange multipliers λ^w and $\lambda^{\frac{\partial w}{\partial n}}$ are expressed by linear combinations of the same Lagrange interpolants, $\mathbf{N} = \{ N_1 \quad N_2 \quad \dots \}$:

$$\lambda^w = \mathbf{N} \boldsymbol{\lambda}^w \qquad \lambda^{\frac{\partial w}{\partial n}} = \mathbf{N} \boldsymbol{\lambda}^{\frac{\partial w}{\partial n}} \quad (7)$$

were the column vectors $\boldsymbol{\lambda}^w$ and $\boldsymbol{\lambda}^{\frac{\partial w}{\partial n}}$ collect the associated weights.

Stationarity of the variational principle (6), $\delta \Pi_I = 0$, is:

$$\frac{\partial \Pi_I}{\partial \mathbf{u}} \delta \mathbf{u} + \frac{\partial \Pi_I}{\partial \boldsymbol{\lambda}^w} \delta \boldsymbol{\lambda}^w + \frac{\partial \Pi_I}{\partial \boldsymbol{\lambda}^{\frac{\partial w}{\partial n}}} \delta \boldsymbol{\lambda}^{\frac{\partial w}{\partial n}} = 0 \quad (8)$$

which leads, for arbitrary variations of $\delta \mathbf{u}$, $\delta \boldsymbol{\lambda}^w$ and $\delta \boldsymbol{\lambda}^{\frac{\partial w}{\partial n}}$, to the standard form

$$\begin{bmatrix} \mathbf{K} & \mathbf{G}^w & \mathbf{G}^{\frac{\partial w}{\partial n}} \\ \mathbf{G}^{wT} & & \\ \mathbf{G}^{\frac{\partial w}{\partial n}T} & \mathbf{0} & \end{bmatrix} \begin{Bmatrix} \mathbf{u} \\ \boldsymbol{\lambda}^w \\ \boldsymbol{\lambda}^{\frac{\partial w}{\partial n}} \end{Bmatrix} = \begin{Bmatrix} \mathbf{f} \\ \mathbf{q}^w \\ \mathbf{q}^{\frac{\partial w}{\partial n}} \end{Bmatrix} \quad (9)$$

The domain integrals are

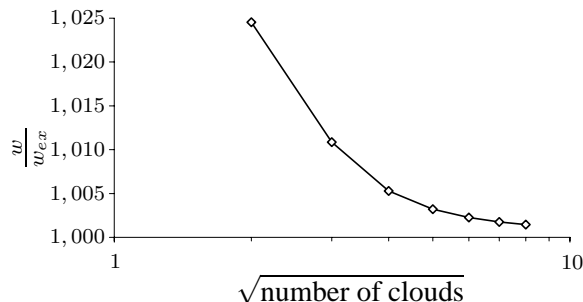


Figure 1: Normalized central displacement.

$$\mathbf{K} = \int_{\Omega} \mathbf{B}^T \mathbf{D} \mathbf{B} d\Omega$$

$$\mathbf{f} = \int_{\Omega} \Phi^T \bar{p} d\Omega + \int_{\bar{V}_n} \Phi^T \bar{V}_n d\Gamma_{\bar{V}_n} + \int_{\bar{M}_n} \left(-\frac{\partial \Phi^T}{\partial n} \right) \bar{M}_n d\Gamma_{\bar{M}_n}$$

where $\mathbf{B} = -(\mathbf{L}\nabla)\Phi$ and the essential boundary conditions are

$$\mathbf{G}^w = - \int_{\Gamma_{\bar{w}}} \Phi^T \mathbf{N} d\Gamma_{\bar{w}} \qquad \mathbf{q}^w = - \int_{\Gamma_{\bar{w}}} \mathbf{N}^T \bar{w} d\Gamma_{\bar{w}}$$

$$\mathbf{G}^{\frac{\partial w}{\partial n}} = - \int_{\Gamma_{\frac{\partial w}{\partial n}}} \frac{\partial \Phi^T}{\partial n} \mathbf{N} d\Gamma_{\frac{\partial w}{\partial n}} \qquad \mathbf{q}^{\frac{\partial w}{\partial n}} = - \int_{\Gamma_{\frac{\partial w}{\partial n}}} \mathbf{N}^T \frac{\partial \bar{w}}{\partial n} d\Gamma_{\frac{\partial w}{\partial n}}$$

Numerical examples

The numerical tests here presented concern a square simply supported plate of which only a quarter was analysed due to symmetry. The following data was used: length, $a = 2,0$ m, thickness $t = 0,1$ m, Young’s modulus $E = 30 \cdot 10^6$ kN/m², Poisson’s ratio $\nu = 0,3$ and uniform load $\bar{p} = 10,0$ kN/m. The same number of clouds was assumed for both directions and the background cell nodes (necessary for the integrations) coincide with the position of the center of the *clouds*. Gauss-Legendre quadrature with six points on each direction was used. For the interpolation of the Lagrange multipliers linear Lagrange shape functions were considered. The plate was analysed for different numbers of clouds with constant radius, $h_{\alpha} = 2a$, and for the first two terms of the enrichment series, $M_{\alpha} = 2$. Results (normalized central displacement) are shown in Fig. 1.

Conclusions

The numerical implementation of the *hp*-clouds method to thin plates was presented. The possibility of accurately representing continuous derivatives of a prescribed order, thus generating *a priori* smooth stress fields, and the use of Trefftz or T-functions as the enrichment functions were the main motivations for this work. Implementation aspects like the order of the quadrature used, the number of points used to impose the essential boundary conditions and the use of *p* refinement need further investigation.

Acknowledgments

This work has been partially supported by FCT through projects "Financiamento Plurianual" and POCTI/33066/ECM/2000.

References

- [1] I. Babuška and J. M. Melenk. The Partition of Unity Method. *Int. J. Num. Meth. Eng.*, 40:727–758, 1997.
- [2] T. Belytschko, Y. Krongauz, D. Organ, M. Fleming, and P. Krysl. Meshless methods: An overview and recent developments. *Comput. Methods Appl. Mech. Engrg.*, 139:3–47, 1996.
- [3] C. A. Duarte. *The Hp Cloud Method*. PhD thesis, Faculty of the Graduate School of the University of Texas at Austin, 1996.
- [4] O. Garcia, E. A. Fancello, C. S. Barcellos, and C. A. Duarte. *hp*-clouds in mindlin's thick plate model. *Int. J. Num. Meth. Eng.*, 47:1381–1400, 2000.
- [5] V.M.A. Leitão. A meshless method for Kirchhoff plate bending problems. *Int. J. Num. Meth. Eng.*, 52:1107–1130, 2001.
- [6] Carlos Tiago. Utilização e desenvolvimento de uma formulação indirecta de trefftz na análise de lajes finas. Master's thesis, Inst. Sup. Técnico, 1998.
- [7] K. Washizu. *Variational Methods in Elasticity and Plasticity*. Pergamon Press, second edition, 1975.

Exact transformation of domain integrals into boundary integrals in anisotropic plate bending problems

E. L. Albuquerque¹, P. Sollero¹, W. S. Venturini², and M. H. Aliabadi³

¹Faculty of Mechanical Engineering, State University of Campinas
13083-970, Campinas, Brazil, sollero@fem.unicamp.br

²São Carlos School of Engineering, University of São Paulo
13566-590, São Carlos, Brazil, venturin@sc.usp.br

³Engineering Department, Queen Mary College, University of London
E1 4NS, London, UK, M.H.Aliabadi@qmw.ac.uk

Keywords: boundary element method, laminate composite material, plate bending, Kirchhoff's theory.

Abstract. This paper presents a boundary element formulation without any domain integral for general anisotropic plate bending with loads applied transversely in the plate surface. The domain integral, which comes from loads transversely applied in an area of plate surface, are transformed into boundary integral by exact transformation. Uniformly and linearly distributed loads are considered. A numerical example concerning orthotropic plate bending problems is presented. Results show good agreement when compared with analytical solutions available in literature.

Introduction

In general plate bending boundary element method, domain integrals arise in the formulation due to the distributed load in the domain (see for example Aliabadi [1]). In order to evaluate these integrals, cell integration scheme can give accurate results, as carried out by Shi and Bezzine [2] for anisotropic plate bending problems. However, the discretization of the domain into cells reduces the advantage of boundary element method in that only the boundary of the problem needs to be discretized into elements.

In this work, domain integrals which come from distributed loads are transformed into boundary integrals by exact transformation using the radial integration method. This method was initially presented by Venturini [3] in 1988 for isotropic plate bending problems. The most attractive feature of the method is its simplicity since only the radial variable is integrated.

For domain integrals which include unknown variables, the proposed procedure can be performed using radial basis function as in the dual reciprocity method (Gao [4]).

Boundary integral equation for bending problems of anisotropic plates

Using Rayleigh-Green identity, an integral equation for an anisotropic thin plate under transversal load $g(p)$ can be written as (see Shi and Bezine [2]):

$$Kw(Q) + \int_{\Gamma} \left[V_n^* w - m_n^* \frac{\partial w}{\partial n} \right] d\Gamma + \sum_{i=1}^{N_c} R_{c_i}^* w_{c_i} = \int_{\Gamma} \left[V_n w^* - m_n \frac{\partial w^*}{\partial n} \right] d\Gamma + \sum_{i=1}^{N_c} R_{c_i} w_{c_i}^* + \int_{\Omega} g w^* d\Omega, \quad (1)$$

where n is the outward unit normal vector to the boundary Γ , m_n , V_n are respectively the normal bending moment and the Kirchhoff's equivalent shear force on the boundary Γ , R_c is thin plate reactions of corners, w_c is the deflexion of corners, P is the source point, Q is the field point, and the symbol "*" stands for the fundamental solutions.

The constant K is introduced in order to consider that the point Q can be in the domain, on the boundary, or outside the domain. If the point Q is on a smooth boundary, than $K = 1/2$.

Transformation of domain integrals into boundary integrals in anisotropic plate bending problem

Consider a plate under loading g , applied in a Ω_g area. Assuming that loading g has a linear distribution $(Ax + By + C)$ in the area Ω_g , the domain integral can be written as:

$$\int_{\Omega_g} g w^* d\Omega = \int_{\Omega_g} (Ax + By + C) w^* \rho d\rho d\theta \quad (2)$$

or

$$\int_{\Omega_g} g w^* d\Omega = \int_{\theta} \int_0^r (Ax + By + C) w^* \rho d\rho d\theta, \quad (3)$$

where r is the value of ρ in a point of boundary Γ_g .

Defining F^* as the following integral:

$$F^* = \int_0^r (Ax + By + C)w^* \rho d\rho, \tag{4}$$

we can write:

$$\int_{\Omega_g} gw^* d\Omega = \int_{\theta} F^* d\theta. \tag{5}$$

Considering an infinitesimal angle $d\theta$ (Figure 1), the relation between the arch length $rd\theta$ and the infinitesimal boundary length $d\Gamma$, can be written as:

$$\cos \alpha = \frac{r \frac{d\theta}{2}}{\frac{d\Gamma}{2}}, \tag{6}$$

or

$$d\theta = \frac{\cos \alpha}{r} d\Gamma. \tag{7}$$

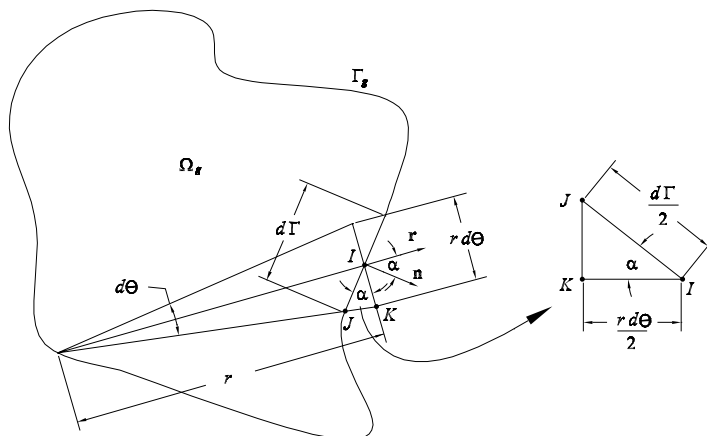


Figure 1: Transformation of domain integral into boundary integral.

Using the properties of internal product of unity vectors \mathbf{n} and \mathbf{r} , indicated in Figure 1, we can write:

$$d\theta = \frac{\mathbf{nr}}{r} d\Gamma. \quad (8)$$

Finally, substituting equation (8) into equation (5), the domain integral of equation (1) can be written as boundary integral given by:

$$\int_{\Omega_g} gw^* d\Omega = \int_{\Gamma_g} \frac{F^*}{r} \mathbf{nr} d\Gamma. \quad (9)$$

Provided that

$$x = \rho \cos \theta \quad (10)$$

and

$$y = \rho \sin \theta, \quad (11)$$

the integral F^* can be written as

$$F^* = \int_0^r \frac{1}{8\pi} (A\rho \cos \theta + B\rho \sin \theta + C) [C_1 R_1 + C_2 R_2 + C_3 (S_1 - S_2)] \rho d\rho, \quad (12)$$

where C_1 , C_2 , and C_3 are the same functions of equation (12) Equation (12) can be rewritten as:

$$F^* = \frac{1}{8\pi} \left\{ (A \cos \theta + B \sin \theta) \int_0^r \rho^2 [C_1 R_1 + C_2 R_2 + C_3 (S_1 - S_2)] d\rho + C \int_0^r \rho [C_1 R_1 + C_2 R_2 + C_3 (S_1 - S_2)] d\rho \right\}. \quad (13)$$

Numerical results

Consider a square plate of side length $a = 1$ m and thickness $h = 0.01$ m. The material is orthotropic and its material properties are: $E_x = 2.068 \cdot 10^{11}$ Pa, $E_y = E_x/15$, $\nu_x = 0.3$, $G_{xy} = 6.055 \cdot 10^8$ Pa. The square plate is considered simply supported on its four edges under uniformly distributed load $q = 1$ Pa applied along its domain (Figure 2). For this case the results obtained by BEM will be compared with the solution obtained by

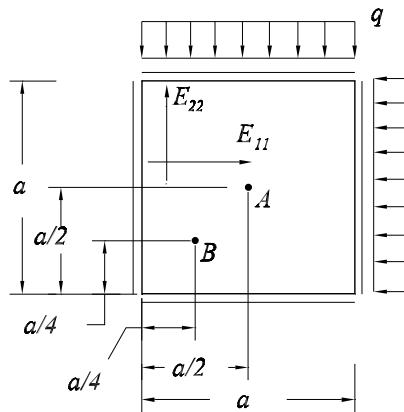


Figure 2: Square plate with simply-supported edges under uniformly distributed load.

Timoshenko and Woinowski-Krieger [5] which solve this problem using a series solution.

In order to assess convergency, the problem is solved using different meshes and the results for deflexions at point A and at point B are compared with series solutions using $N = 19$ and $M = 19$. This series solution for point A is $w_{se.} = 8.1258 \cdot 10^{-7}$ m and for point B is $w_{se.} = 4.5211 \cdot 10^{-7}$ m. Table shows deflexions computed by the present BEM technique using different meshes and their respective errors compared to Timoshenko and Woinowski-Krieger [5] series solutions.

Table 1: Accuracy of deflexions obtained by BEM for different number of elements (NE) of the orthotropic square plate with simply supported edges under uniformly distributed loads.

NE	Deflexions and errors			
	w at A [m]	Er. at A [%]	w at B [m]	Er. at B [%]
8	$9.22 \cdot 10^{-7}$	13.45	$5.40 \cdot 10^{-7}$	19.38
16	$8.04 \cdot 10^{-7}$	1.03	$4.58 \cdot 10^{-7}$	1.35
24	$8.04 \cdot 10^{-7}$	1.01	$4.46 \cdot 10^{-7}$	1.25
32	$8.06 \cdot 10^{-7}$	0.77	$4.47 \cdot 10^{-7}$	1.09
40	$8.08 \cdot 10^{-7}$	0.59	$4.52 \cdot 10^{-7}$	0.88

As it can be seen in Table , results are very poor when 8 elements (2 elements per side) are used. However, they converge fastly to the series solutions if the number of the element is increased. When 40 boundary elements are used, deflexions in both points present errors below 1 % if compared with series solutions.

Conclusions

In this work, the use of radial transformation in boundary element formulation for the analysis of anisotropic plate bending problems was presented. Domain integrals which come from linearly and uniformly distributed loads were transformed into boundary integrals by exact radial transformation. A numerical example was shown for orthotropic materials. The numerical results obtained with the present BEM technique were compared with results obtained analytically and show good agreement.

Aknowlegment

The authors would like to thank to FAPESP (The State of São Paulo Research Foundation) for the financial support of this work.

References

- [1] M. H. Aliabadi. *Boundary element method, application in solids and structures*. John Wiley, New York, 2002.
- [2] G. Shi and G. Bezzine. A general boundary integral formulation for the anisotropic plate bending problems. *J. Composite Materials*, 22:694–716, 1988.
- [3] W. S. Venturini. *A study of boundary element method and its application on engineering problems*. PhD thesis, University of São Paulo, São Carlos School of Engineering, 1988. In Portuguese.
- [4] X. Gao. The radial integration method for evaluation of domain integrals with boundary only discretization. *Engn. Analysis with Boundary Elements*, 26:905–916, 2002.
- [5] S. Timoshenko and S. Woinowski-Krieger. *Theory of Plates and shells*. McGraw-Hill, New York, 1959.

The BEM for Large Deflection Analysis of Plates with Variable Thickness

M.S. Nerantzaki and J.T. Katsikadelis

School of Civil Engineering, National Technical University of Athens,
Zografou Campus, 157173, Athens, Greece
e-mail: jkats@central.ntua.gr

Keywords: Plates, large deflections, nonlinear, elasticity, variable thickness, boundary elements, analog equation method

Abstract. The BEM is developed for large deflection analysis of plates with arbitrary thickness variation law and shape. The problem is formulated in terms of the displacements. The solution is based on the AEM (Analog Equation Method), which converts the three coupled nonlinear differential equations to three uncoupled linear ones, two Poisson's equations and a biharmonic equation under fictitious sources, which are solved using the BEM. The presented numerical results demonstrate the efficiency and accuracy method.

Introduction

Although there is an extensive literature on plates with constant thickness, a rather limited amount of technical literature is available on plates with non-uniform thickness. The reason for this is that the governing differential equation has variable coefficients, and this fact increases the difficulty of the solution. The problem becomes more complicated when large deflections are considered, where the response of the plate is governed by three coupled nonlinear partial differential equations with variable coefficients and therefore the conventional direct BEM can not be applied. In this paper the BEM is developed for large deflection analysis of plates with arbitrary thickness variation law. The solution is based on the concept of the analog equation [1,2], according to which the three coupled nonlinear differential equations are replaced with three uncoupled linear ones, two linear membrane (Poisson's) equations for the membrane displacements and a plate (biharmonic) equation for the transverse displacement subjected to fictitious loads. The fictitious loads are approximated by radial basis functions series and are evaluated using a procedure based on the BEM. Subsequently, displacements and their derivatives, thus the stress resultants, are evaluated from their integral representations, which are used as mathematical formulae. The presented numerical results demonstrate the accuracy and the effectiveness of the AEM tool for the solution of difficult engineering problems.

Problem statement and governing equations

Consider a thin elastic plate of variable thickness, $h = h(x, y)$, occupying the two-dimensional domain Ω with boundary $\Gamma = \cup_{k=1}^K \Gamma_k$ (Fig. 1) and subjected to transverse load $g(x, y)$.

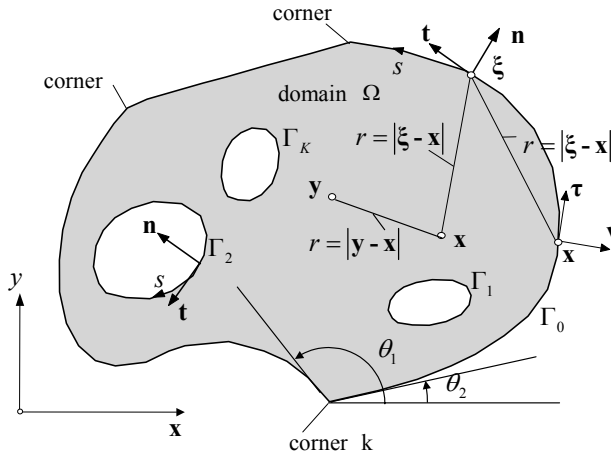


Figure 1: Plate geometry and notation.

Assuming nonlinear kinematical relations (von-Kármán theory), that is

$$\varepsilon_x = u_{,x} + \frac{1}{2}w_{,x}^2, \quad \varepsilon_y = v_{,y} + \frac{1}{2}w_{,y}^2, \quad \gamma_{xy} = u_{,y} + v_{,x} + w_{,x}w_{,y} \quad (1a,b,c)$$

the equilibrium of a plate element yields the following differential equations

$$\left\{ C \left[\left(u_x + \frac{1}{2}w_x^2 \right) + \nu \left(v_y + \frac{1}{2}w_y^2 \right) \right] \right\}_{,x} + \left\{ C \frac{(1-\nu)}{2} (u_y + v_x + w_x w_y) \right\}_{,y} = 0 \quad (2a)$$

$$\left\{ C \frac{(1-\nu)}{2} (u_y + v_x + w_x w_y) \right\}_{,x} + \left\{ C \left[\left(v_y + \frac{1}{2}w_y^2 \right) + \nu \left(u_x + \frac{1}{2}w_x^2 \right) \right] \right\}_{,y} = 0 \quad (2b)$$

$$\begin{aligned} & \nabla^2 (D \nabla^2 w) - (1-\nu)(D_{xx}w_{yy} - 2D_{xy}w_{xy} + D_{yy}w_{xx}) \\ & - C \left\{ \left[\left(u_x + \frac{1}{2}w_x^2 \right) + \nu \left(v_y + \frac{1}{2}w_y^2 \right) \right] w_{xx} \right. \\ & \left. + (1-\nu)(u_y + v_x + w_x w_y)w_{xy} + \left[\left(v_y + \frac{1}{2}w_y^2 \right) + \nu \left(u_x + \frac{1}{2}w_x^2 \right) \right] w_{yy} \right\} = g \end{aligned} \quad (2c)$$

subjected to the general boundary conditions

$$\gamma_1 u + \gamma_2 T x = \gamma_3, \quad \delta_1 v + \delta_2 T y = \delta_3 \tag{3a,b}$$

$$\alpha_1 w + \alpha_2 V^*(w) = \alpha_3, \quad \beta_1 w_n + \beta_2 M^*(w) = \beta_3 \tag{3c,d}$$

$$c_{1l} w + c_{2l} \llbracket T^*(w) \rrbracket_l = c_{3l}, \quad c_{2l} \neq 0 \tag{3e}$$

where $u(x, y)$, $v(x, y)$ are the membrane displacements and $w(x, y)$ the transverse one; $C = Eh / (1 - \nu^2)$, $D = Eh^3 / 12(1 - \nu^2)$ are the variable membrane and bending stiffness of the plate; T_x , T_y the in-plane boundary tractions, $\alpha_i, \beta_i, \gamma_i, \delta_i$ functions specified on Γ and $\llbracket T^*(w) \rrbracket_l$ is the discontinuity jump at l corner and $M^*(w)$, $V^*(w)$, $T^*(w)$ are the normal boundary bending moment, effective shear force and the twisting moment given as

$$M^* = -D[\nabla^2 w + (\nu - 1)(\frac{\partial^2 w}{\partial s^2} + \kappa \frac{\partial w}{\partial n})] \tag{4a}$$

$$V^* = -D[\frac{\partial}{\partial n} \nabla^2 w - (\nu - 1)(\frac{\partial}{\partial s}(\frac{\partial^2 w}{\partial n \partial s} - \kappa \frac{\partial w}{\partial s}))] + \frac{\partial D}{\partial s}(\nu - 1)(\frac{\partial^2 w}{\partial n \partial s} - \kappa \frac{\partial w}{\partial s}) - \frac{\partial D}{\partial n}[\nabla^2 w + (\nu - 1)(\frac{\partial^2 w}{\partial s^2} + \kappa \frac{\partial w}{\partial n})] + T_x \frac{\partial w}{\partial x} + T_y \frac{\partial w}{\partial y} \tag{4b}$$

$$T^* = D(1 - \nu)(\frac{\partial^2 w}{\partial s \partial n} - \kappa \frac{\partial w}{\partial s}) \tag{4c}$$

with $\kappa = \kappa(s)$ being the boundary curvature.

The AEM as boundary-only method

The boundary value problem described by eqs (2) and (3) is solved using the AEM. Assume that u , v and w is the sought solution. If the Laplacian operator is applied to u , v and the biharmonic to w , we obtain

$$\nabla^2 u = b_1(x, y), \quad \nabla^2 v = b_2(x, y), \quad \nabla^4 w = b_3(x, y) \tag{5a,b,c}$$

Eqs (4) indicate that the solution of the original problem could obtained from the solution of these equation under the same boundary conditions, if $b_i(x, y)$, ($i = 1, 2, 3$) were first established. This is possible and is achieved as follows.

We set

$$b_i = \sum_{j=1}^M a_j^i f_j, \quad f_j = f_j(r), \quad r \equiv r_{j\mathbf{x}} = \|\mathbf{x} - \mathbf{x}_j\| \tag{6}$$

and we write the solution of eqs (5) in integral form. Thus, for points \mathbf{x} where the boundary is smooth, we obtain the integral equations [3]

$$\varepsilon u(\mathbf{x}) = -\int_{\Gamma} (u^* u_n - u_n^* u) ds + \sum_{j=1}^M \left[a_j^{(1)} \int_{\Omega} u^* f_j(r) d\Omega \right] \quad (7a)$$

$$\varepsilon v(\mathbf{x}) = -\int_{\Gamma} (u^* v_n - u_n^* v) ds + \sum_{j=1}^M \left[a_j^{(2)} \int_{\Omega} u^* f_j(r) d\Omega \right] \quad (7b)$$

$$\begin{aligned} \varepsilon w(\mathbf{x}) = & \int_{\Gamma} \{ \Lambda_1(w^*) V^*(w) + \Lambda_2(w^*) w + \Lambda_3(w^*) M^*(w) + \Lambda_4(w^*) w_n \} ds \\ & + (\nu - 1) \sum_{l=1}^L [w^*(\ln D)_{,s} [\kappa w - w_{,n}]_{,l}] + \sum_{j=1}^M \left[a_j^{(3)} \int_{\Omega} w^* f_j(r_j) d\Omega \right] \end{aligned} \quad (7c)$$

$$\begin{aligned} \varepsilon w_{,\nu}(\mathbf{x}) = & \int_{\Gamma} \{ K_1(w_{,\nu}^*) V^*(w) + K_2(w_{,\nu}^*) w + K_3(w_{,\nu}^*) M^*(w) + K_4(w_{,\nu}^*) w_n \} ds \\ & (\nu - 1) \sum_{l=1}^L (w_{,\nu}^*(\ln D)_{,s} [\kappa w - w_{,n}]_{,l}) + \sum_{j=1}^M \left(a_j^{(3)} \int_{\Omega} w_{,\nu}^* f_j(r_j) d\Omega \right) \end{aligned} \quad (7d)$$

$u^* = (1/2\pi) \ln r$, $w^* = (1/8\pi) r^2 \ln r$ are the fundamental solution of Laplace and biharmonic equation; $\Lambda_k(w^*)$, $K_k(w_{,\nu}^*)$, ($k = 1, 2, 3, 4$) known kernels and $\varepsilon = 1, 1/2, 0$ depending on whether point \mathbf{x} inside Ω , on Γ or outside Ω . The domain integrals in eqs (7) are converted to boundary line integrals using the Green and Rayleigh-Green identities as described in [4,5]. The displacements derivatives inside Ω result by direct differentiation of eqs (7a)-(7c)

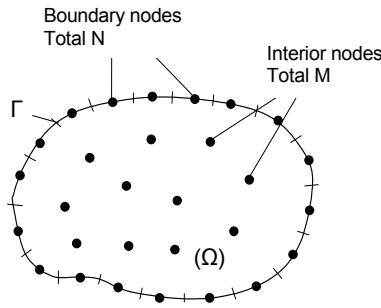


Figure 2: Boundary discretization and domain nodal points

Numerical implementation

Using N constant elements to approximate the line integrals and M meshless domain collocation points (Fig. 2), eqs (3a-3d) and (7) yield $8N$ equations with

$8N + 3M$ unknowns, namely $8N$ boundary values $u, u_n, w, w_n, M^*(w), V^*(w)$ and $3M$ coefficients $a_j^i \ i = 1, 2, 3 \ j = 1, 2, \dots, M$. The additional $3M$ equations are obtained by collocating eqs (2) at the M interior nodal points and substituting the involved derivatives. Subsequent elimination of the boundary quantities yields the following system of $3M$ non linear algebraic equations

$$\mathbf{F}_1(\mathbf{a}^{(1)}, \mathbf{a}^{(2)}, \mathbf{a}^{(3)}) = 0, \quad \mathbf{F}_2(\mathbf{a}^{(1)}, \mathbf{a}^{(2)}, \mathbf{a}^{(3)}) = 0, \quad \mathbf{F}_3(\mathbf{a}^{(1)}, \mathbf{a}^{(2)}, \mathbf{a}^{(2)}) = \mathbf{g} \quad (8)$$

from which the coefficients $\mathbf{a}^{(1)}, \mathbf{a}^{(2)}, \mathbf{a}^{(2)}$ are established. Finally, the displacements and their derivatives at any point are evaluated from the respective integral representations

Numerical results

On the basis of the solution procedure described in the previous sections a FORTRAN code has been written and numerical results have been obtained. The employed radial basis functions are multiquadrics, $f_j(r) = \sqrt{r^2 + c^2}$. An optimum value of the shape parameter c was estimated from the stationary value of the total potential $\Pi(c)$ of the plate [3].

Example. A circular plate of radius a under uniform load g and thickness variation law $h = h_0 \exp[\beta(r/a)^2]$, $r \leq a$ has been analyzed. The results for the deflection are presented in Table 1. The lower values for $\beta = 0$ are obtained from approximate formulae [7].

Table 1. Central deflection w/h_0 in a circular plate ($\nu = 0.3$).

β		Clamped immovable			Simply supported movable		
		$\alpha = g(a/h_0)^4 / E$			$\alpha = g(a/h_0)^4 / E$		
		1	3	5	5	7	10
-0.4	AEM	0.2847	0.6666	0.9027	2.107	2.450	2.845
	Ref[6]	0.2711	0.6334	0.8596			
-0.2	AEM	0.2209	0.5641	0.7973	1.951	2.284	2.668
	Ref[6]	0.2195	0.5564	0.7847			
0	AEM	0.1680	0.4588	0.6796	1.800	2.121	2.492
	Ref[7]	0.1680	0.4588	0.6808			
0.2	AEM	0.1265	0.3608	0.5576	1.650	1.961	2.319
	Ref[6]	0.1268	0.3634	0.5648			
0.4	AEM	0.0950	0.2777	0.4430	1.499	1.800	2.148
	Ref[6]	0.0966	0.2838	0.4555			

Conclusions

The boundary element method has been developed for large deflection analysis of plates with variable thickness

- The proposed method is based on the concept of the analog equation, which converts the three coupled nonlinear partial equations with variable coefficients to three uncoupled simple linear differential equations, namely 2 membrane equations and 1 linear plate equation with constant thickness.
- The method is boundary-only in the sense the discretization and integration is performed only on the boundary. With respect to domain nodal points the method is meshless. Therefore the method maintains all advantages of pure BEM
- The deflections and the stress resultants are computed at any point using the respective integral representation as mathematical formulas.
- Accurate numerical results for the displacements and the stress resultants are computed.
- The concept of the analog equation in conjunction with radial basis functions approximation of the fictitious sources renders the BEM a versatile computational method for solving difficult nonlinear engineering problems

References

- [1] J.T. Katsikadelis and M.S. Nerantzaki *Engineering Analysis with Boundary Elements*, **23**, 363-. (1999).
- [2] J.T. Katsikadelis and C.G. Tsiatas *Engineering Analysis with Boundary Elements*, **25**, 655-667, (2001).
- [3] J.T. Katsikadelis and A.J. Yiotis *Journal of Engineering Mathematics*, (to appear) (2003).
- [4] J.T. Katsikadelis *Boundary Elements: Theory and Applications*, Elsevier, (2002).
- [5] J.T. Katsikadelis and A.E. Armenakas *ASME, Journal of Applied Mechanics*, **56**, 364-374, (1989).
- [6] Ye Jianqiao *Applied Mathematical Modelling*, **55**, 325-328, (1991).
- [7] C.Y. Chia *Nonlinear Analysis of Plates*, McGraw-Hill, (1980).

Shear Deformable Plate Buckling by the Boundary Element Method

J. Purbolaksono and M. H. Aliabadi

*Department of Engineering, Queen Mary, University of London,
Mile End Road, London E1 4NS*

Abstract

In this paper the boundary element method formulation for buckling analysis of Reissner plate is presented. Plate buckling equations are written as a standard eigenvalue problem. Buckling coefficients and buckling modes are obtained using this formulation. The boundary is discretised into quadratic isoparametric element and the domain is discretised using constant cells. Some examples are presented, and the results show good agreements with analytical and finite element results.

1. Introduction

Buckling analysis of compression panels has become particularly important in engineering structures. Buckling phenomenon of structure members in compression has been investigated by researchers analytically, experimentally and numerically. Analytical solutions of plate buckling based on the classical plate theory can be found in [1] [3]. Numerical method such as the finite element method (FEM) has been used by many researchers to investigate the problems. Experiment of works on buckling can be found in a review of plate buckling research [2]. Solutions for typical loading of buckling model as shown in Figure 1.1 can be found in many references.

More recently, the boundary element method (BEM) has provided a powerful solution to the field of plate buckling. Syngellakis and Elzein [4], extended a boundary element solution of the plate buckling based on Kirchhoff theory to accommodate any combination of loadings and support conditions. Nerantzaki and Katsidelakis [5], developed a BEM-based

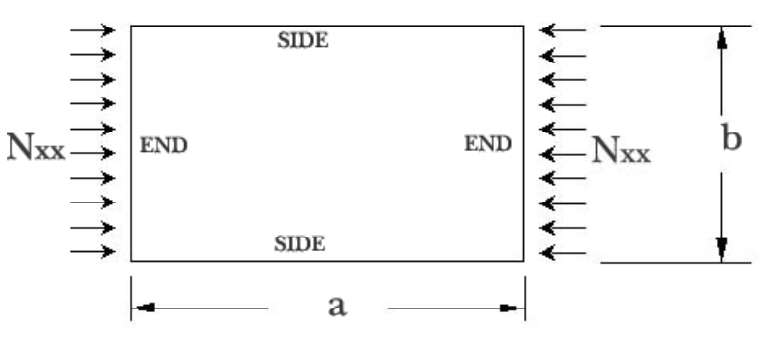


Figure 1.1: Typical buckling model

method for plate buckling analysis of plates with variable thickness. Elastic buckling analysis of plates using boundary element can also be found in [6].

In this paper the derivation of boundary integral equations for the buckling analysis of the Reissner shear deformable plate are developed. Plate buckling equations are written as a standard eigenvalue problem. The formulation is formed by coupling boundary element formulations of shear deformable plate and two dimensional plane stress elasticity. The domain integrals which appear in this formulation are discretised using constant cells. The eigenvalue problem of plate buckling yields a critical load factor and buckling modes.

2. Boundary Integral Equations

At present work, determination of in-plane stress resultants in the domain is the first step solution to the analysis of plate buckling. Next, the plate buckling problem equations are derived from the plate bending equations. Critical load factors are introduced into the equations as multiplying factors of body forces.

2.1. Boundary Integral Equation of In-plane Stress Resultants

The in-plane stress resultants at domain points X' are written as

$$N_{\alpha\beta}^{linear}(X') = \int_{\Gamma} U_{\Delta\alpha\beta}^*(X', x)t_{\Delta}(x)d\Gamma(x) - \int_{\Gamma} T_{\Delta\alpha\beta}^*(X', x)u_{\Delta}(x)d\Gamma(x) \tag{2.1}$$

The fundamental solutions $U_{\Delta\alpha\beta}^*$ and $T_{\Delta\alpha\beta}^*$ can be found in [7].

2.2. Boundary Integral Formulation of Plate Buckling Problem

The plate bending equation is transformed into the equivalent plate buckling formulation by introducing critical load factor λ as follows:

$$\begin{aligned}
 & C_{ij}(x')w_i(x') + \int_{\Gamma} P_{ij}^*(x', x)w_j(x)d\Gamma(x) \\
 = & \int_{\Gamma} W_{ij}^*(x', x)p_j^{linear}(x)d\Gamma(x) \\
 & + \lambda \int_{\Omega} W_{i3}^*(x', X)[q + (N_{\alpha\beta}^{linear}w_{3,\beta})_{,\alpha}](X)d\Omega(X) \quad (2.2)
 \end{aligned}$$

where the terms $C_{ij}(x')$ are equal to $\frac{1}{2}\delta_{ij}$ when x' is located on a smooth boundary.

The deflection equation w_3 at the domain points X' is required as the additional equation to arrange an eigenvalue equation, as follows:

$$\begin{aligned}
 w_3(X') = & \int_{\Gamma} W_{3j}^*(X', x)p_j^{linear}(x)d\Gamma(x) - \int_{\Gamma} P_{3j}^*(X', x)w_j(x)d\Gamma(x) \\
 & + \lambda \int_{\Omega} W_{33}^*(X', X)[q + (N_{\alpha\beta}^{linear}w_{3,\beta})_{,\alpha}](X)d\Omega(X) \quad (2.3)
 \end{aligned}$$

To arrange an eigenvalue equation, the derivative quantities have to be expressed in terms of $w_3(X)$ by making use of a radial basis function [8]. The kernel solutions P_{ij}^* and W_{ij}^* can also be found in [7].

3. Numerical Procedure

In this section, the numerical procedure of plate buckling analysis by a boundary element method is presented. The first step is to solve boundary integral of in-plane problem and calculate the stress resultants at the domain points. The second step is to solve boundary integral formulation of buckling problem.

3.1. Determination of the in-plane stresses

As presented in [7], once the boundary integral equation of in-plane displacement has been solved, the stresses N_{11} , N_{12} , and N_{22} at domain points

(equation 2.1) can be calculated. The stresses are required to solve the plate buckling problem.

3.2. Solving plate buckling problem

After applying boundary conditions into the equation (2.2), then it can also be written as a system of algebraic equation in terms of known and unknown quantities, gives:

$$[\mathbf{B}]_{3N \times 3N} \{\mathbf{Y}\}_{3N} = \lambda [\mathbf{K}]_{3N \times L} \{\mathbf{w}_3\}_L \quad (3.1)$$

The $q(X)$ quantities in the equations (2.2) and (2.3) are set to zero. N and L are number of boundary elements and domain points, respectively.

The equation (2.3) also can be written in matrix form as follows:

$$[\mathbf{I}] \{\mathbf{w}_3\}_L = [\mathbf{BB}]_{L \times 3N} \{\mathbf{Y}\}_{3N} + \lambda [\mathbf{KK}]_{L \times L} \{\mathbf{w}_3\}_L \quad (3.2)$$

where matrix $[\mathbf{I}]$ is an identity matrix. The matrices $[\mathbf{B}]$ and $[\mathbf{BB}]$ contain coefficient matrices related to the fundamental solutions. The matrices $[\mathbf{K}]$ and $[\mathbf{KK}]$ are obtained by multiplication of the fundamental solution, in-plane stresses $N_{\alpha\beta}$ at domain points and approximation function.

Substituting equation (3.1) into equation (3.2), the equation can be written as a standard eigenvalue problem equation as follows:

$$([\psi] - \frac{1}{\lambda} [\mathbf{I}]) \{\mathbf{w}_3\}_L = 0 \quad (3.3)$$

where $[\psi] = [\mathbf{BB}]_{L \times 3N} [\mathbf{B}]_{3N \times 3N}^{-1} [\mathbf{K}]_{3N \times L} + [\mathbf{KK}]_{L \times L}$.

Buckling analysis of shear deformable plates has been presented as a standard eigenvalue problem. Buckling modes correspond to the eigenvalue problem can be obtained .

4. Numerical Examples

4.1. Simply supported rectangular plate under uni-axial load

This example presents the buckling coefficients of the simply supported plate with different aspect ratio a/b (length to width of plate). The values for the buckling coefficients are compared with Timoshenko's solution [1]. The buckling modes are shown in Figure 4.2

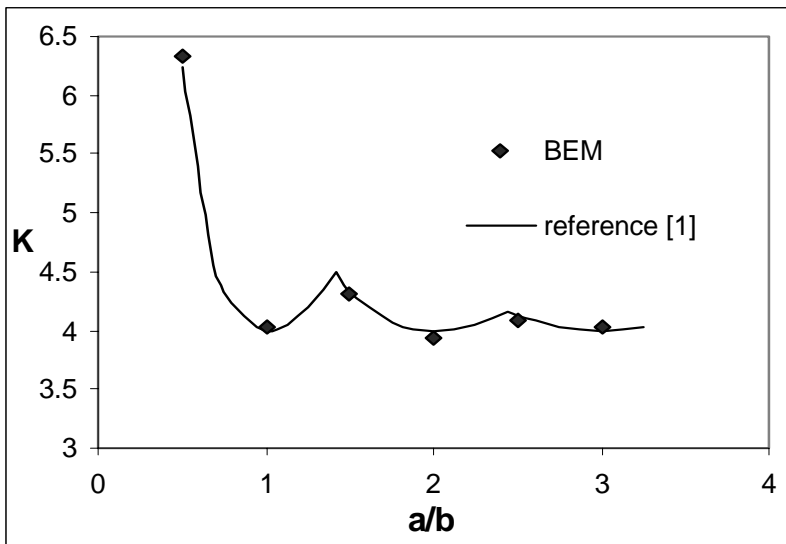


Figure 4.1: Buckling coefficients of simply supported rectangular plate

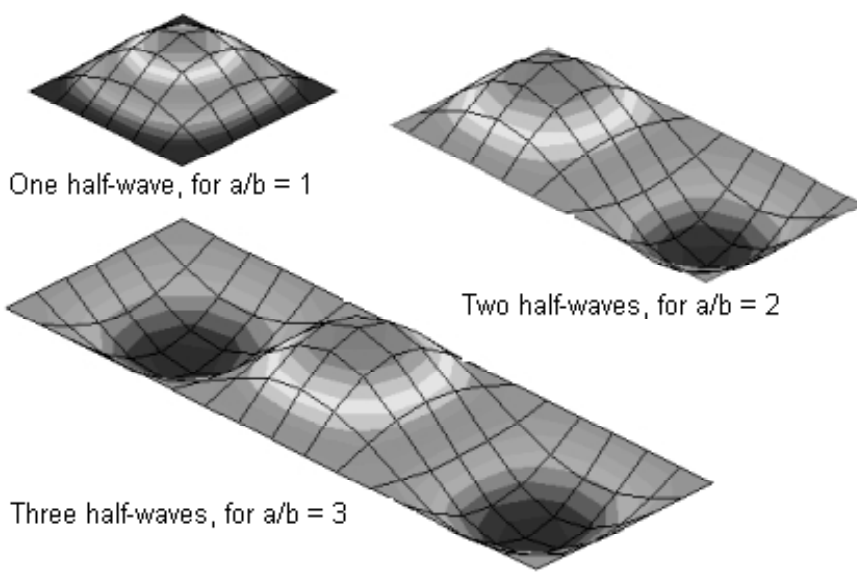


Figure 4.2: Buckling modes of simply supported rectangular plate

4.2. Square plate with different boundary conditions subjected to uni-axial loads

Buckling coefficients of square plate subjected uni-axial loads with different boundary conditions (see Figure 1.1 for the loading conditions). The results are compared with the FEM results using I-DEAS software package [9].

Tabel 4.1 Buckling coefficient of square plate subjected to uni-axial loads

Boundary condition	K (BEM)	K (FEM)
A	10.387	10.392
B	7.757	7.796
C	6.972	7.014
D	1.724	1.739

A : sides and ends clamped

B : sides clamped, ends simply supported

C : ends clamped, sides simply supported

D : one side free, one side clamped, ends simply supported

5. Conclusion

In this paper buckling analysis of shear deformable plate by the boundary element method was presented. Some numerical examples are presented and shown to be good agreements with analytical and finite element results.

Acknowledgement

This work was supported by Queen Mary College Research Studentship, University of London. The authors wish to thank Tatacipta Dirgantara for many useful discussions.

References

- [1] Timoshenko, S. and Gere, J.M., *Theory of Elastic Stability*, second edition, McGraw-Hill, New York (1961)
- [2] Walker, A.C., *A Brief Review of Plate Buckling Research*, In: Rhodes J, Spence J, editors, *Behaviour of Thin-walled Structures*, Elsevier, London (1984)

- [3] Brush, D.O. and Almorh, B.O., *Buckling of Bars, Plates and Shells*, McGraw-Hill, New York (1975)
- [4] Syngellakis, S. and Elzein, A., *Plate Buckling Loads by the Boundary Element Method*, Int. J. Numer. Meth. Engng. **37**, 1763-1778 (1994)
- [5] Nerantzaki, M.S. and Katsikadelis, J.T., *Buckling of Plates with Variable Thickness — An Analog Equation Solution*, Engineering Analysis with Boundary Element, **18**, pp 149-154 (1996)
- [6] Lin, J., Duffield, R.C. and Shih, H., *Buckling Analysis of Elastic Plates by Boundary Element Method*, Engineering Analysis with Boundary Element, **23**, pp 131-137 (1999)
- [7] Dirgantara, T., *Boundary Element Analysis of Crack in Shear Deformable Plates and Shells*, Ph.D Thesis, Department of Engineering, Queen Mary and Westfield College, University of London (2000)
- [8] Wen, P.H., Aliabadi, M.H. and Young, A., *Plane Stress and Plate Bending Coupling in BEM analysis of Shallow Shells*, Int. J. Numer. Meth. Engng. **48**, 1107-1125 (2000)
- [9] Lawry, M.H., *I-DEAS Master Series: Student Guide*, Structural Dynamics Research Corporation, Milford, Ohio (1998)